

Mixing effects of light and heavy rare earths in the Laves phase compounds $\text{Nd}_{1-x}\text{HR}_x\text{Co}_2$
(HR = Gd,Tb)

This article has been downloaded from IOPscience. Please scroll down to see the full text article.

2003 J. Phys.: Condens. Matter 15 5599

(<http://iopscience.iop.org/0953-8984/15/32/319>)

View [the table of contents for this issue](#), or go to the [journal homepage](#) for more

Download details:

IP Address: 171.66.16.125

The article was downloaded on 19/05/2010 at 15:02

Please note that [terms and conditions apply](#).

Mixing effects of light and heavy rare earths in the Laves phase compounds $\text{Nd}_{1-x}\text{HR}_x\text{Co}_2$ (HR = Gd, Tb)

Z W Ouyang¹, G H Rao¹, H F Yang¹, W F Liu¹, G Y Liu¹, X M Feng¹
and J K Liang^{1,2}

¹ Institute of Physics and Centre for Condensed Matter Physics, Chinese Academy of Sciences, Beijing 100080, People's Republic of China

² International Centre for Materials Physics, Academia Sinica, Shenyang 110015, People's Republic of China

E-mail: ghrao@aphy.iphy.ac.cn

Received 12 May 2003

Published 1 August 2003

Online at stacks.iop.org/JPhysCM/15/5599

Abstract

The mixing effects of light and heavy rare earths in cubic Laves phase compounds $\text{Nd}_{1-x}\text{HR}_x\text{Co}_2$ (HR = Gd, Tb) have been investigated by means of x-ray powder diffraction and magnetic measurements. In $\text{Nd}_{1-x}\text{Tb}_x\text{Co}_2$, the saturation moment M_S exhibits an anomaly and could be ascribed to an abrupt jump of the Co moment at a critical concentration $x_c \approx 0.33$, whereas, in $\text{Nd}_{1-x}\text{Gd}_x\text{Co}_2$, M_S does not show such an anomaly and a relatively simple magnetic behaviour is observed at $x_c \approx 0.43$. The different behaviours of these two systems can be understood by considering the structural distortion of a cubic unit cell at low temperature. A field-induced metamagnetic transition from weak ferrimagnetism to strong ferrimagnetism is observed in both systems. This can be interpreted by the evolution of magnetization with the help of percolation theory. The compensation points are observed in both systems, which are well explained within the two-sublattice model. A double peak of the AC susceptibility observed in $\text{Nd}_{1-x}\text{Tb}_x\text{Co}_2$ near $x_0 \approx 0.19$ does not necessarily mean the occurrence of a first-order phase transition. The observed second-order magnetic phase transition near x_0 can be well described by Landau theory of the phase transition.

1. Introduction

The cubic Laves phase RCo_2 (R = rare earth), as a subject of great interest for more than 20 years, exhibits a number of characteristic properties, e.g. variable moment on the Co atom, first-order magnetic transition, applied or molecular field induced metamagnetic transition (MMT)

of the Co sublattice, etc. Owing to its simple crystal structure and intriguing characteristics, RCo_2 is an ideal system for checking physical theories of magnetism.

YCo_2 and LuCo_2 are known as strong exchange-enhanced paramagnetic materials and undergo a MMT under an external magnetic field of 69 and 74 T, respectively [1, 2]. By replacing Co with Al and Ga, a significant reduction in critical field H_c for the transition and the onset of weak ferromagnetism have been observed in these compounds [3, 4]. However, in the RCo_2 based on magnetic lanthanides, it was found that the Co moment can be induced by the molecular field exerted by a localized 4f moment. Owing to the negative exchange constant of the f–d interaction, compounds with light rare-earth (LR) elements are ferromagnetic. Both the molecular field on Co sites $H_{\text{mol}}^{\text{Co}}$ and the Co moment M_{Co} are parallel to the external field H_{ext} . Substitution of Y for LR can lead to the $H_{\text{mol}}^{\text{Co}}$ being less than H_c . An applied field will easily bring pseudo-binary compounds $\text{LR}_{1-x}\text{Y}_x\text{Co}_2$ with $H_{\text{mol}}^{\text{Co}} < H_c$ to the MMT. For the heavy rare earths (HR), the HR moment is aligned antiparallel to the Co moment and both $H_{\text{mol}}^{\text{Co}}$ and M_{Co} are accordingly antiparallel to H_{ext} . Replacing HR with Y or Lu decreases $H_{\text{mol}}^{\text{Co}}$ and can lead to a collapse of the Co moment, which corresponds to the so-called inverse MMT [5, 6]. In addition, the magnetic phase transition of RCo_2 is second order for $\text{R} = \text{Gd}$, Tb and Tm , but is first order for $\text{R} = \text{Dy}$, Ho and Er [7–9]. Bloch *et al* [7] used an exchange-enhanced paramagnetism model to explain the mechanism of the magnetic phase transition in RCo_2 . Inoue and Shimizu [8] later proposed an improved version of this theory for the phase transition in RCo_2 . Recently, Khmelevsky and Mohn [9] suggested a different explanation for the change of the order of the magnetic transition in RCo_2 over the full rare-earth series on the basis of fixed-spin-moment band structure calculations of the isostructural compound YCo_2 at different lattice constants.

The magnetic properties of the compounds with a mixture of LR and HR are expected to show some unusual behaviour. On the one hand, it was reported recently that the Al-based Laves phase compounds $\text{Sm}_{1-x}\text{Gd}_x\text{Al}_2$ exhibit a spin–orbital compensation point at about 85 K when $x = 0.0185$ [10]. It was proposed that such a compensation point is driven by the different temperature dependence of the spin and orbital moments [11]. On the other hand, the magnetic properties of the Co-based compounds $\text{LR}_{1-x}\text{HR}_x\text{Co}_2$ have scarcely been discussed in the literature. In fact, the magnetic properties of the Co sublattice in RCo_2 compounds are strongly influenced by the amount and nature of the rare earth. It has been suggested that, going from HR to LR compounds, both the magnetization of the Co sublattice and the interaction between the rare-earth spin and the Co spin are enhanced [12, 13]. Therefore, it seems of interest to investigate the properties of compounds with a mixture of LR and HR.

In this paper we make a comparative investigation of the mixing effects in $\text{Nd}_{1-x}\text{HR}_x\text{Co}_2$ ($\text{HR} = \text{Gd}$, Tb). The choice of rare earth is based on the following considerations:

- (i) NdCo_2 has an easy magnetization direction (EMD) of [110] at 4.2 K and an orthorhombic distortion is observed [14].
- (ii) The HR is chosen to have a different EMD from the LR. In TbCo_2 , the EMD is along [111] and owns a much larger anisotropic magnetostriction [15]. However, in GdCo_2 the EMD is along [100] at 4.2 K and exhibits a low magnetostriction due to the spherical 4f electron shell of the Gd^{3+} ion ($L = 0$) [15].

The difference of anisotropy between Tb^{3+} and Gd^{3+} ions is expected to show some different magnetic properties between $\text{HR} = \text{Gd}$ and Tb in $\text{Nd}_{1-x}\text{HR}_x\text{Co}_2$.

The present paper is organized as follows. Section 2 describes experimental details. Section 3 presents the experimental results. Section 4 is concerned with a discussion of the magnetic properties of $\text{Nd}_{1-x}\text{HR}_x\text{Co}_2$ ($\text{HR} = \text{Gd}$, Tb). Conclusions are given in section 5.

2. Experimental details

Polycrystalline samples of $\text{Nd}_{1-x}\text{HR}_x\text{Co}_2$ with $x = 0.0\text{--}1.0$ (step = 0.1), 0.06, 0.13, 0.16, 0.23, 0.26, 0.36, 0.41–0.49 (step = 0.01) for HR = Gd, and with $x = 0.1\text{--}1.0$ (step = 0.1), 0.14–0.26 (step = 0.01), 0.31–0.38 (step = 0.01) for HR = Tb were prepared by arc melting of stoichiometric amounts of constituting elements Nd, Gd, Tb and Co with a purity better than 99.9% under a protective argon atmosphere. Appropriate excess amounts of the rare-earth metal were added to compensate the weight loss during arc melting and subsequent heat treatment. The ingots were melted several times to ensure homogeneity. Samples thus obtained were sealed in an evacuated quartz tube and homogenized at 1073 K for 14 days. To avoid possible phase transformation during cooling, the quartz tube was quenched in water.

X-ray powder diffraction (XRD) data were collected by a Rigaku Rint-2500 diffractometer with Cu $K\alpha$ radiation. The temperature dependence of the lattice constant of the samples with $x = 0.40$ and 0.43 for HR = Gd, and 0.17 and 0.18 for HR = Tb, were derived from XRD experiments from about 85 to 300 K. Curves of magnetization versus temperature of the samples were measured by using a vibrating sample magnetometer in a field of 0.05 T, from which the Curie temperature can be derived by extrapolating M^2 to zero. The field dependence of the magnetization of the samples at 5 K was measured by a superconducting quantum interference device (SQUID) magnetometer. The AC magnetic susceptibility was measured by a mutual inductance bridge with a fixed frequency of 240 Hz.

3. Experimental results

3.1. Structure and lattice constant

XRD analysis shows that all of the samples $\text{Nd}_{1-x}\text{HR}_x\text{Co}_2$ (HR = Gd, Tb) are cubic Laves phase with the MgCu_2 -type structure (space group $Fd\bar{3}m$). The lattice constant a at room temperature, as given in figure 1(a), decreases with increasing HR concentration. This can be ascribed to the smaller radius of the HR atom than that of the Nd atom. For $\text{Nd}_{1-x}\text{Tb}_x\text{Co}_2$, the concentration dependence of a approximately follows Vegard's law by $a = xa_1 + (1 - x)a_0$, where a_0 and a_1 are the lattice constants of NdCo_2 and TbCo_2 , respectively. For the compounds $\text{Nd}_{1-x}\text{Gd}_x\text{Co}_2$, the a - x curve exhibits a kink at $x = 0.6$. Since the Curie temperature of $\text{Nd}_{1-x}\text{Gd}_x\text{Co}_2$ is above room temperature for $x > 0.6$, the kink can be attributed to a transition from a non-magnetic to magnetic state with increasing Gd concentration at room temperature.

3.2. The Curie temperature and saturation moment

The Curie temperatures T_C of $\text{Nd}_{1-x}\text{HR}_x\text{Co}_2$ (HR = Gd, Tb) obtained by extrapolating M^2 to zero were plotted in figure 1(b). The dependence of T_C on the HR concentration indicates a linear variation in both systems. The field dependences of the magnetization at 5 K measured by the SQUID magnetometer are illustrated in figure 2. For the sake of comparison, the data for HR = Tb taken from [18] are also plotted. In $\text{Nd}_{1-x}\text{Tb}_x\text{Co}_2$, with the increase in Tb concentration, the magnetization reduces for the samples of $x \leq 0.3$, whereas for $x \geq 0.4$ the magnetization increases. There exists a field-induced magnetic transition in the composition range of $x = 0.3\text{--}0.8$. At $x = 0.3$, the required field H_c is about 0.5 T. A further increase in Tb concentration reduces H_c . In $\text{Nd}_{1-x}\text{Gd}_x\text{Co}_2$, a similar variation of magnetization is observed. However, a field-induced magnetic transition is observed only at $x = 0.4$ with an H_c of about 0.3 T. According to the law of the approach to saturation, by extrapolating $1/H$ to zero on the linear part of the M versus $1/H$ curves, the concentration dependence of the saturation moment

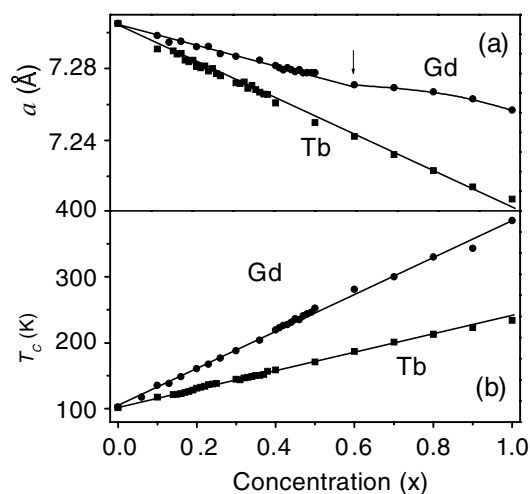


Figure 1. The concentration dependences of lattice constant a at room temperature and Curie temperature T_c of $\text{Nd}_{1-x}\text{HR}_x\text{Co}_2$ (HR = Gd, Tb). The arrow indicates the kink. For HR = Tb, the data for $x = 0$ – 1.0 (step = 0.1) are taken from [18].

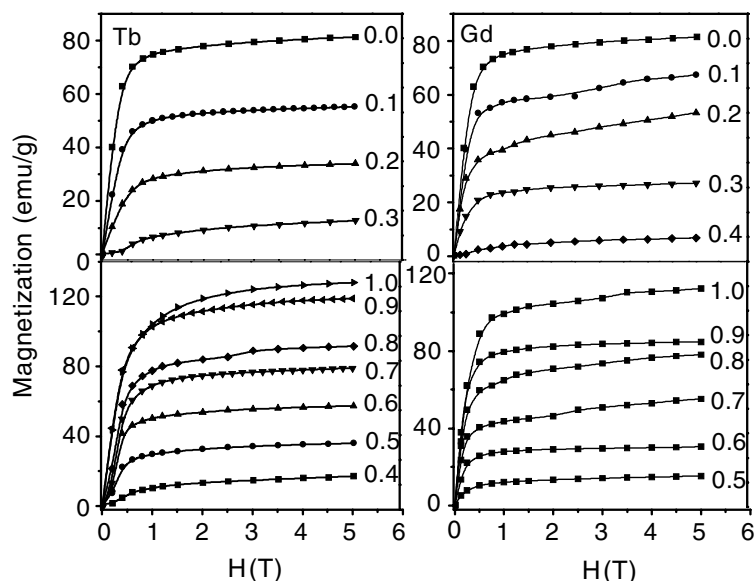


Figure 2. The field dependence of magnetization at 5 K of $\text{Nd}_{1-x}\text{HR}_x\text{Co}_2$ (HR = Gd, Tb). The data for HR = Tb are taken from [18].

M_S is derived and shown in figure 3. M_S varies almost linearly with concentration on both Nd- and HR-rich sides. A minimum of M_S occurs at a critical concentration of $x_c \approx 0.33$ and 0.43 for Tb and Gd, respectively. It should be noticed that the magnetization measurements have been carried out using powder samples. M versus H curves reveal that an applied field less than 0.5 T will lead to the arrangement of R and Co sublattices along the external field. With the increase of H_{ext} , one can expect to obtain a collinear arrangement of sublattices along the direction of the external field, i.e. EMD. Therefore, the value of M_S obtained up to 5 T reflects the magnetization along EMD, to a large degree.

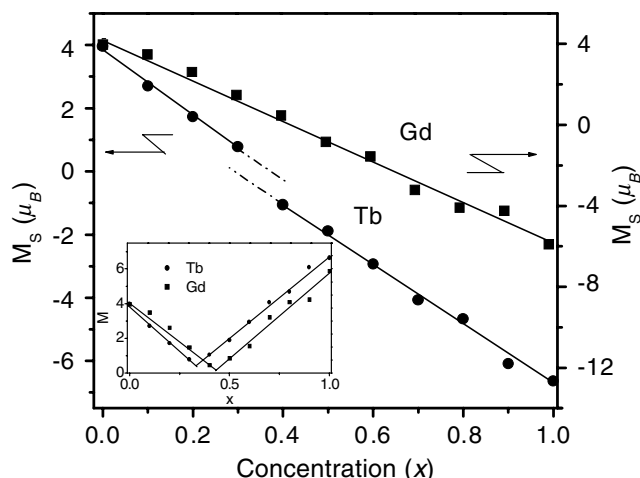


Figure 3. The concentration dependence of saturation moment M_S at 5 K of $\text{Nd}_{1-x}\text{HR}_x\text{Co}_2$ (HR = Gd, Tb), in which M_S is taken as negative for HR-rich compounds. The circles are the data taken from [18].

Swift and Wallace [16] investigated the magnetic characteristics of a series of $\text{R}'_x\text{R}''_{1-x}\text{Al}_2$ compounds with the cubic Laves phase (R' and R'' are two different rare earths) and concluded that, in the magnetically ordered state, spins of the trivalent rare earths always couple ferromagnetically, i.e. the magnetic moments align parallel if both are LRs or HRs, whereas the moments align antiparallel if R' is a LR and R'' is a HR or vice versa. In the $\text{R}'_x\text{R}''_{1-x}\text{Co}_2$ compounds, since the crystallographic environment of the Co atoms around the rare-earth ions does not change with x , it is reasonable to assume that the magnetic characteristics of the rare-earth sublattice mimic that in the $\text{R}'_x\text{R}''_{1-x}\text{Al}_2$ compounds. According to the results of [16], taking the saturation moment of HR-rich compounds as negative, figure 3 indicates a jump of M_S in the vicinity of x_c for $\text{Nd}_{1-x}\text{Tb}_x\text{Co}_2$, whereas such behaviour is not evident for $\text{Nd}_{1-x}\text{Gd}_x\text{Co}_2$. It is accepted that an abrupt change in magnetic moment can be related to the value of magnetovolume anomaly: $\omega_s = (V_m - V_0)/V_0$, where V_m and V_0 denote the crystal volumes in the magnetic and non-magnetic states, respectively. Within a first-order approximation, ω_s is related to the d-electron magnetic moment μ_d by $\omega_s = kC\mu_d^2$, where k is the isotropic compressibility and C is the magnetovolume coupling constant [17]. Our early study on the magnetovolume effect in compounds $\text{Nd}_{1-x}\text{Tb}_x\text{Co}_2$ showed that the anomaly of M_S could be attributed to an abrupt change of the Co moment at x_c [18]. The calculation of ω_s from figure 4 for $\text{Nd}_{1-x}\text{Gd}_x\text{Co}_2$ reveals that ω_s is about 2.7×10^{-3} for $x = 0.40$ and 2.4×10^{-3} for $x = 0.43$ at 86 K, which suggests that the Co moment also undergoes a jump in the vicinity of $x_c \approx 0.43$. Nevertheless, such a jump is relatively small compared to that in the compounds $\text{Nd}_{1-x}\text{Tb}_x\text{Co}_2$, leading to a negligible anomaly of M_S under present experimental conditions.

3.3. Magnetic properties around x_c

The field dependences of magnetization at 5 K of $\text{Nd}_{1-x}\text{HR}_x\text{Co}_2$ (HR = Gd, Tb) around x_c are presented in figure 5. All samples exhibit a low magnetization. In $\text{Nd}_{1-x}\text{Tb}_x\text{Co}_2$, a field-induced magnetic transition is clearly observed for $x = 0.31, 0.32, 0.37$ and 0.38 . According to [18], such a transition, including that of $x = 0.3$ – 0.8 in figure 2, is a MMT from

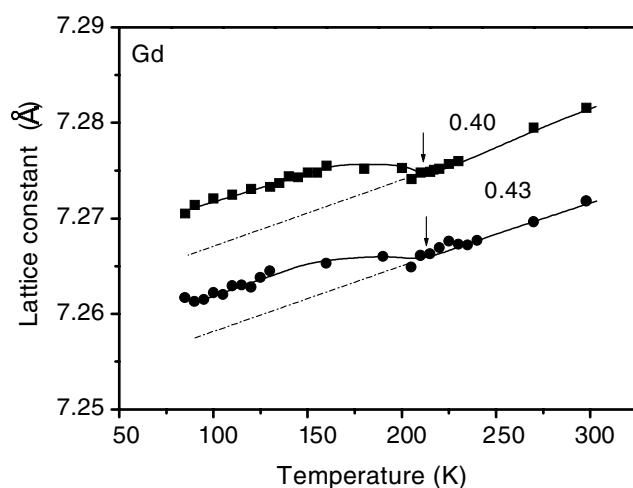


Figure 4. The temperature dependence of the lattice constant a (± 0.001 Å) of $\text{Nd}_{1-x}\text{Gd}_x\text{Co}_2$ ($x = 0.40, 0.43$). The arrows show the T_C .

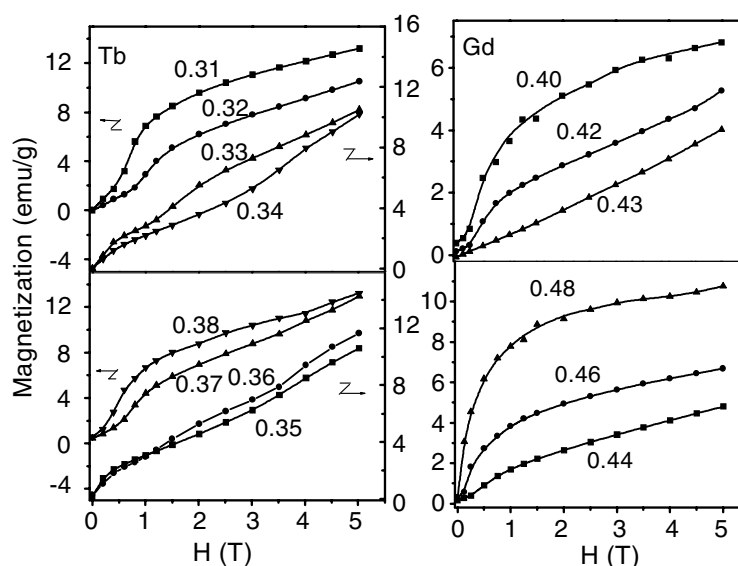


Figure 5. The field dependence of magnetization at 5 K of $\text{Nd}_{1-x}\text{HR}_x\text{Co}_2$ (HR = Gd, Tb) near the critical concentration x_c .

weak ferrimagnetism to strong ferrimagnetism with a required field smaller than 1.0 T. The M versus H curves near x_c , i.e. $x = 0.33$ – 0.35 , exhibit a complex behaviour, where two or more steps are observed. In comparison with Tb, a relatively simple magnetic behaviour is observed in compounds $\text{Nd}_{1-x}\text{Gd}_x\text{Co}_2$. The magnetization varies almost linearly with field for $x = 0.43$. A MMT is observed only at $x = 0.40, 0.42, 0.44$ and 0.46 .

Within the two-sublattice model, due to the different temperature dependences of the total moment of the R sublattice M_R and the moment of the Co sublattice M_{Co} , one may expect that M_R and M_{Co} will compensate at some temperature T_{comp} below T_C . The temperature

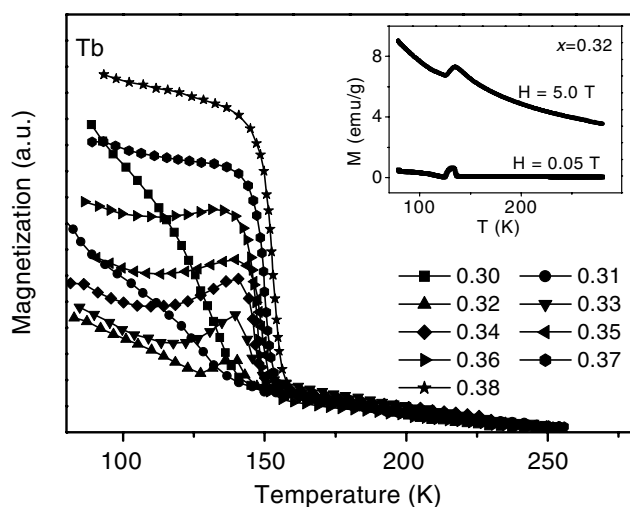


Figure 6. The temperature dependence of magnetization at 0.05 T of $\text{Nd}_{1-x}\text{Tb}_x\text{Co}_2$ near $x_c \approx 0.33$. The inset is the M versus T curves for $x = 0.32$ measured by a SQUID magnetometer at 0.05 and 5.0 T, respectively.

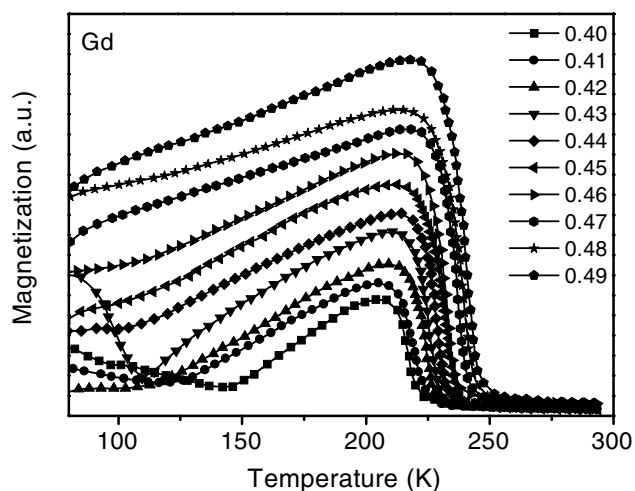


Figure 7. The temperature dependence of magnetization at 0.05 T of $\text{Nd}_{1-x}\text{Gd}_x\text{Co}_2$ near $x_c \approx 0.43$.

dependences of the magnetization of $\text{Nd}_{1-x}\text{Tb}_x\text{Co}_2$ with $x = 0.30$ – 0.38 , and $\text{Nd}_{1-x}\text{Gd}_x\text{Co}_2$ with $x = 0.40$ – 0.49 are illustrated in figures 6 and 7, respectively. A compensation point is observed in both systems. In $\text{Nd}_{1-x}\text{Tb}_x\text{Co}_2$, the temperature of compensation T_{comp} is derived to be 125–110 K for $x = 0.32$ – 0.36 and decreases with the increase of Tb concentration. The M versus T curve of $x = 0.32$ measured by the SQUID magnetometer indicates that the compensation point still exists in a high field of 5.0 T and shows a stable character, as illustrated in the inset of figure 6. Accordingly, in $\text{Nd}_{1-x}\text{Gd}_x\text{Co}_2$, T_{comp} varies from 143 to 110 K for $x = 0.40$ – 0.43 and also shows a decrease with the increase in Gd concentration. Such a compensation point is a characteristic of weak ferrimagnetism, in which M_R aligns

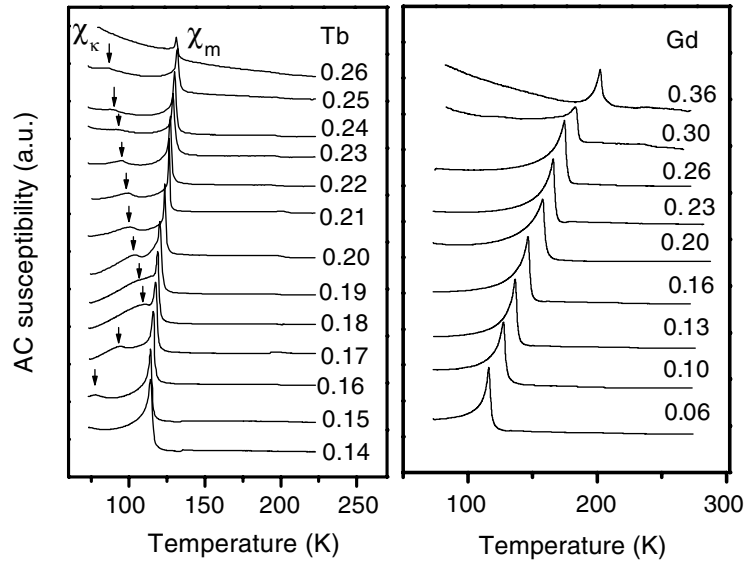


Figure 8. The temperature dependence of AC susceptibility at 240 Hz of $\text{Nd}_{1-x}\text{HR}_x\text{Co}_2$ (HR = Gd, Tb) near the critical concentration x_0 .

antiparallel to and almost equal to M_{Co} [19]. Far from the critical concentration x_c , M_{R} is much larger than M_{Co} or vice versa. The temperature dependence of the magnetization is mainly contributed by that of M_{R} or M_{Co} , leading to the absence of a compensation point. It should be noticed that the compensation point observed in our systems is different from the spin–orbital compensation point in $\text{Sm}_{1-x}\text{Gd}_x\text{Al}_2$, where a compensation point is driven by the different temperature dependence of the spin and orbital moments [10, 11].

3.4. Magnetic phase transition

According to the results of $\text{R}'_x\text{R}''_{1-x}\text{Al}_2$ reported by Swift and Wallace [16], it is reasonable to assume that the total moment of the R sublattice M_{R} varies linearly with the HR concentration in $\text{Nd}_{1-x}\text{HR}_x\text{Co}_2$ (HR = Gd, Tb). Taking $\mu_{\text{Nd}} = 2.1 \mu_{\text{B}}$ [20], $\mu_{\text{Tb}} = 8.9 \mu_{\text{B}}$ and $\mu_{\text{Gd}} = 7.0 \mu_{\text{B}}$ [21], M_{R} would approach zero at $x_0 \approx 0.19$ for $\text{Nd}_{1-x}\text{Tb}_x\text{Co}_2$ and $x_0 \approx 0.23$ for $\text{Nd}_{1-x}\text{Gd}_x\text{Co}_2$, respectively. The temperature dependences of AC susceptibility near this critical composition x_0 , as illustrated in figure 8, exhibit a clear change of behaviour near T_{C} . The typical λ -type curve of $\text{Nd}_{1-x}\text{Gd}_x\text{Co}_2$ indicates a second-order magnetic phase transition. However, the curves of $\text{Nd}_{1-x}\text{Tb}_x\text{Co}_2$ are characterized by a double peak χ_{k} (on the low temperature side) and χ_{m} (on the high temperature side) in the vicinity of the magnetic ordering temperature. For $x = 0.17$ and 0.18 , the double peak is very close to each other, which is considered as a character of first-order transition. The characteristic temperature T_{k} corresponding to χ_{k} peak shows a maximum at $x = 0.17$ (see figure 9), on both sides of which the χ_{k} peak becomes weaker and broader and the T_{k} varies linearly with concentration. For RCO_2 compounds the double peak was considered as a characteristic of a first-order transition [22, 23]. However, the gradual change of both magnetization and lattice constant around T_{C} (figure 10) indicates that the magnetic phase transition in our system is essentially a second-order one. The field dependence of magnetization of $x = 0.17$ at different temperatures near T_{C} are presented in figure 11. The Arrott plots obtained by plotting M^2 versus

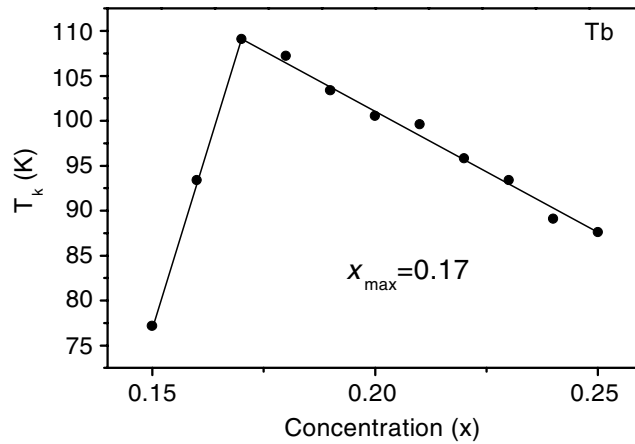


Figure 9. The concentration dependence of the characteristic temperature T_k for χ_k peak in AC susceptibility of $\text{Nd}_{1-x}\text{Tb}_x\text{Co}_2$ ($x = 0.15\text{--}0.25$).

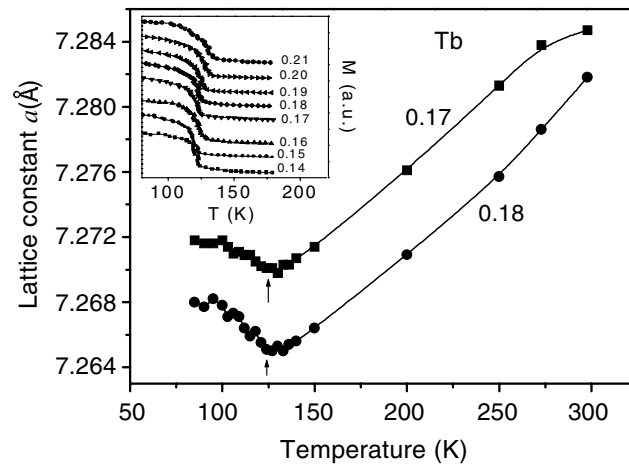


Figure 10. The temperature dependence of lattice constant a (± 0.001 Å) of $\text{Nd}_{1-x}\text{Tb}_x\text{Co}_2$ ($x = 0.17, 0.18$). The arrows show the T_C . The inset plots the M versus T curves for $x = 0.14\text{--}0.21$.

H/M do not display S-shaped curves with two linear parts, corresponding to a MMT from a paramagnetic to ferromagnetic state above T_C , as illustrated in figure 12, which suggests the occurrence of a second-order phase transition at T_C .

According to the Landau theory of second-order phase transition [24, 25], the magnetic free energy of the system can be written as a function of order parameter M , temperature T and external field H , i.e.

$$\phi(M, T, H) = \phi_0(T) + \alpha(T - T_C)M^2 + \beta M^4 - VMH \quad (1)$$

where α and β are functions of temperature and V is the volume of the system. From the equilibrium condition

$$\left[\frac{\partial \phi(M, T, H)}{\partial M} \right]_{H, T} = 0 \quad (2)$$

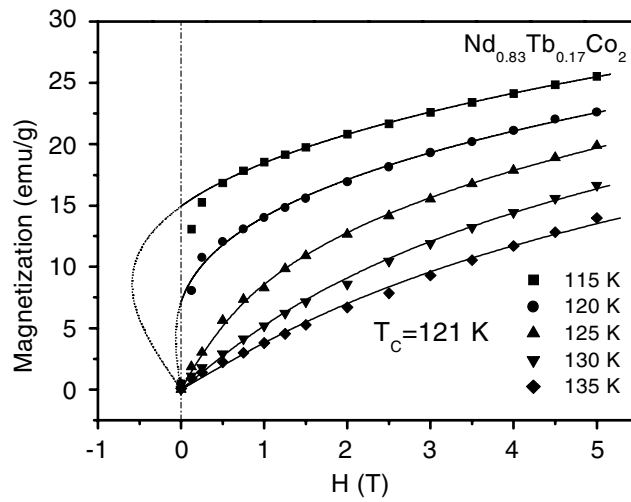


Figure 11. The field dependence of magnetization at different temperatures near $T_C = 121$ K of $\text{Nd}_{0.83}\text{Tb}_{0.17}\text{Co}_2$. The full curves are the results of fitting using the Landau theory of phase transition.

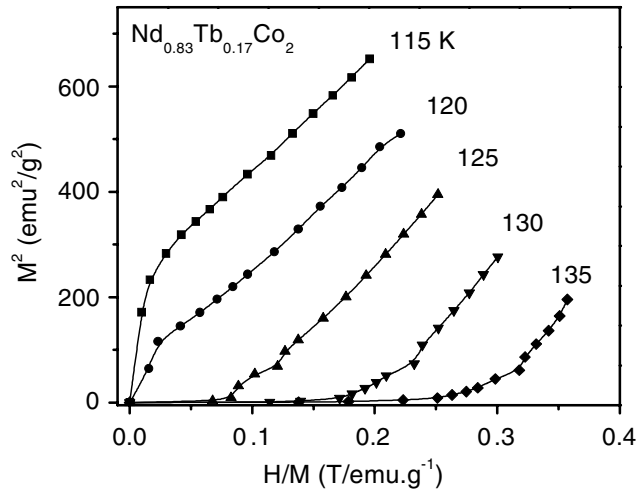


Figure 12. Arrott plots at different temperatures near $T_C = 121$ K of $\text{Nd}_{0.83}\text{Tb}_{0.17}\text{Co}_2$.

the order parameter M as a function of H and T can be derived as

$$2\alpha(T - T_C)M + 4\beta M^3 = VH. \quad (3)$$

Using the experimental field dependence of magnetization at different temperatures, a least-squares fitting gives the fitted curves of M versus H , as illustrated in figure 11. The obtained parameters are given in table 1 and are shown as the inset of figure 13, from which one can see that $\alpha(T - T_C)/V$ shows a linear variation with temperature and has a negative value when $T < T_C$, whereas β/V remains positive and exhibits an anomaly near T_C . Hence, the sign of the fitted parameters meets the condition for a second-order transition. The free energy curve at zero field below T_C , as plotted in figure 13, exhibits a minimum at a definite non-zero M . Noticing that the curve is very similar with that of NdCo_2 obtained by a band structure

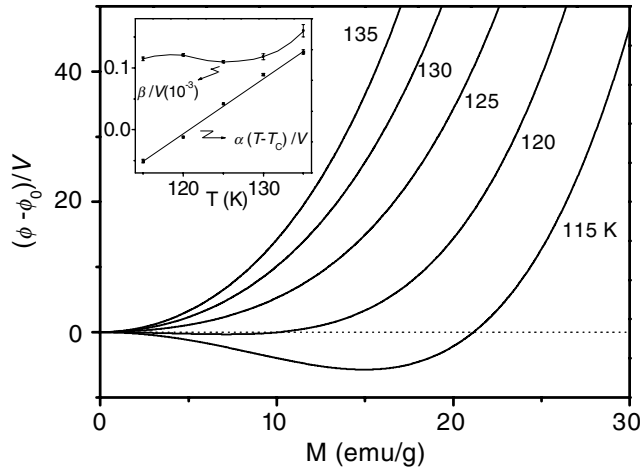


Figure 13. The magnetization dependence of free energy at zero field near T_C for $\text{Nd}_{0.83}\text{Tb}_{0.17}\text{Co}_2$. The inset shows the fitted value of the parameters.

Table 1. The parameters fitted by a least-squares fitting using the Landau theory of the second-order phase transition.

T (K)	115	120	125	130	135
$\alpha(T - T_C)/V$ (T g emu^{-1})	-0.051(3)	-0.012(1)	0.042(1)	0.089(2)	0.126(4)
β/V ($\times 10^{-3}$) ($\text{T g}^3 \text{emu}^{-3}$)	0.115(3)	0.121(2)	0.110(2)	0.118(5)	0.160(10)

calculation at 0 K and NdCo_2 shows a second-order magnetic transition [9], we conclude that $\text{Nd}_{0.83}\text{Tb}_{0.17}\text{Co}_2$ also exhibits a second-order phase transition at its magnetic ordering temperature.

It is inferred from these experimental and theoretical results that there exist some different magnetic properties between $\text{Nd}_{1-x}\text{Tb}_x\text{Co}_2$ and $\text{Nd}_{1-x}\text{Gd}_x\text{Co}_2$ near the critical concentration x_0 . In addition, the observation of a double peak near T_C in RCo_2 compounds does not necessarily mean an occurrence of a first-order magnetic phase transition, in contrast to the early argument [22, 23].

4. Discussion

4.1. Relationship between structure and magnetic properties

In RCo_2 compounds, the Co moment is induced by the molecular field $H_{\text{mol}}^{\text{Co}}$ provided by a 4f moment: $H_{\text{mol}}^{\text{Co}} \propto J_{\text{RCo}}(g - 1)J$, where g is the Landé factor associated with the angular momentum J of the rare earth. The exchange coupling constant J_{RCo} is defined by the exchange energy and the number of nearest neighbours and is therefore closely connected with the length of the R-Co bond [26]. The latter is associated with the change of structure. In a cubic crystal the structure distortion of the cubic unit cell can be related to EMD determined by the magnetocrystalline anisotropy.

Experimentally, NdCo_2 has an EMD of [110] at 4.2 K and undergoes an orthorhombic distortion [14]. TbCo_2 has an EMD of [111] and exhibits a rhombohedral distortion with a much larger anisotropic magnetostriction of $\lambda_{111} = 4.5 \times 10^{-3}$ [15]. However, GdCo_2 shows a tetragonal distortion at low temperature and a low magnetostriction of $\lambda_{100} = -1.2 \times 10^{-3}$

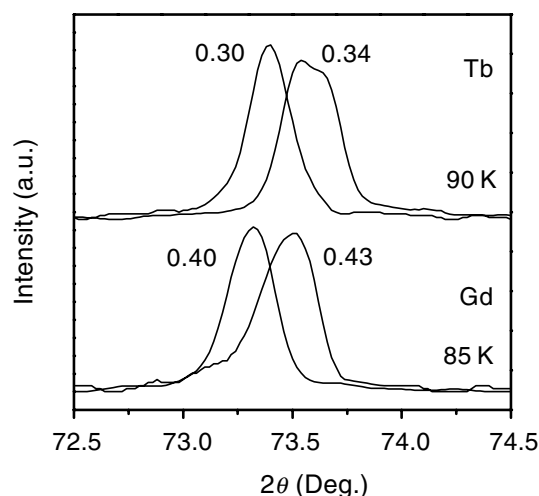


Figure 14. X-ray diffraction patterns of the (440) peak of $\text{Nd}_{1-x}\text{HR}_x\text{Co}_2$ (HR = Gd, Tb) near x_c at 90 and 85 K, respectively.

in its EMD of [100] due to the spherical 4f electron shell of the Gd^{3+} ion ($L = 0$) [15]. In addition, Levitin *et al* [27, 28] found that the EMD of a mixed compound $\text{R}'_x\text{R}''_{1-x}\text{Co}_2$ is the same as that of the predominant rare earth. According to these results, with the increase of HR concentration, the EMD will change from [110] to [111] for $\text{Nd}_{1-x}\text{Tb}_x\text{Co}_2$ and from [110] to [100] for $\text{Nd}_{1-x}\text{Gd}_x\text{Co}_2$, leading to a larger structural distortion in the former than that in the latter, although there probably exists a transition region within a small range of composition. Such a difference of structural transition is also reflected in the splitting of high angle XRD reflections. Figure 14 plots the (440) peak near x_c . The splitting is very clear in $\text{Nd}_{1-x}\text{Tb}_x\text{Co}_2$, which indicates a clear structural transition near x_c . In $\text{Nd}_{1-x}\text{Gd}_x\text{Co}_2$, no discernible splitting of any peaks, including the (440) peak, is observed. Notice that the width of the (440) peak significantly increases at $x = 0.43$ relative to that at $x = 0.40$. This suggests the existence of a relatively small structural transition near x_c . The larger change of the structure in $\text{Nd}_{1-x}\text{Tb}_x\text{Co}_2$ would lead to a larger anomaly of M_S at x_c compared to that in $\text{Nd}_{1-x}\text{Gd}_x\text{Co}_2$. In $\text{Nd}_{1-x}\text{Gd}_x\text{Co}_2$ the anomaly is hardly even observed under present experimental conditions (see figure 3).

According to the atomic model for anisotropic magnetostriction [29, 30], when the EMD changes from [110] to [100] near x_c in $\text{Nd}_{1-x}\text{Gd}_x\text{Co}_2$, due to the high tetrahedral ($43m$) symmetry at R sites, the potentially huge value of λ_{100} is effectively shorted out and exhibits a small value, leading to a small change of bond length of R–Co. Hence, a small change of Co moment is expected so that the anomaly of M_S cannot be observed near x_c . On the other hand, when the EMD changes from [110] to [111] near x_c in $\text{Nd}_{1-x}\text{Tb}_x\text{Co}_2$, a huge λ_{111} is allowed because two inequivalent tetrahedral sites (0, 0, 0) and (1/4, 1/4, 1/4) exist in the C15 structure which permit internal distortion along [111]. This internal distortion lowers the symmetry and drives a huge external rhombohedral distortion, leading to a large change of the length of the R–Co bond. Therefore, a large change of Co moment is expected and the anomaly of M_S can be clearly observed near x_c .

In addition, the effect of a crystalline electric field (CEF) should be taken into account. Neutron diffraction experiments show that CEF plays a role not only for the compounds with Pr, Nd and Sm, but also in the HR compounds [31]. In the HR compounds CEF is not large enough to reduce appreciably the free ion moment, whereas in the LR compounds CEF can

lead to a considerable reduction of the free-ion moment [7]. However, CEF has a similar effect in both systems due to the same LR. Therefore, it is reasonable to assume that the difference of the M_S anomaly at x_c in both systems is not mainly caused by CEF. Within the framework of the single-ion model, the magnetocrystalline anisotropy originates from the electrostatic interaction between the anisotropic 4f electron shell of the R ion and the CEF [15]. Therefore, the effect of CEF on anisotropy is essentially included in the discussion of anisotropy above.

Under this consideration, the giant difference of anisotropy of the Tb and Gd sublattices in $\text{Nd}_{1-x}\text{HR}_x\text{Co}_2$ would be likely to cause the much more complex field dependence of magnetization in $\text{Nd}_{1-x}\text{Tb}_x\text{Co}_2$ than in $\text{Nd}_{1-x}\text{Gd}_x\text{Co}_2$ in the vicinity of x_c (see figure 5). The characteristic peak χ_k observed in AC susceptibility measurements may be associated with a spin reorientation caused by anisotropy. Whenever the R sublattice anisotropy and the Co sublattice anisotropy favour different EMD one may expect the occurrence of a spin reorientation at a given temperature. According to the discussion above, the Tb sublattice has a larger anisotropy than the Gd sublattice in $\text{Nd}_{1-x}\text{HR}_x\text{Co}_2$, leading to the observation of a χ_k peak in $\text{Nd}_{1-x}\text{Tb}_x\text{Co}_2$, but not in $\text{Nd}_{1-x}\text{Gd}_x\text{Co}_2$. The composition of $x = 0.17$, where T_k exhibits a maximum, is very close to the theoretical critical composition $x_0 = 0.19$. However, it is still unknown why there exists a maximum characteristic temperature near this critical composition.

4.2. Evolution of magnetization

Within the two-sublattice mean-field model, the coupling between the R sublattice moment M_R and the Co sublattice moment M_{Co} in $\text{Nd}_{1-x}\text{HR}_x\text{Co}_2$ (HR = Gd, Tb) compounds consists of randomly distributed ferromagnetic coupling between Nd–Co moments and antiferromagnetic coupling between HR–Co moments. In figure 3, for the sake of discussion, the moments of HR-rich compounds are taken as negative values. In fact, the larger one between M_R and M_{Co} will orient along the direction of the external field H_{ext} . When $0 < x < x_0$, the Nd–Co coupling dominates, leading to a ferromagnetic coupling between the moments of the R and Co sublattices. Both M_R and M_{Co} are parallel to the external field H_{ext} . When $x = x_0$, $M_R \approx 0$. When $x_0 < x < x_c$, there exists a strong competition between Nd–Co coupling and HR–Co coupling. M_{Co} is a little larger than M_R , leading to the M_{Co} parallel to H_{ext} whereas M_R is antiparallel to H_{ext} . When $x = x_c$, $M_{\text{Co}} \approx M_R$. For $x_c < x < 1.0$, the HR–Co coupling prevails, resulting in a ferrimagnetic coupling between the moments of HR and Co sublattices. In this case, M_R is larger than M_{Co} , leading to the M_R parallel to H_{ext} , whereas M_{Co} is antiparallel to H_{ext} . Such an evolution of the magnetism with the concentration behaves as a percolation-like transition. M_{Co} changes its direction with respect to the direction of the applied external field only at x_c , which perhaps is the reason why an anomaly is observed at x_c but not at x_0 .

According to this picture, in the vicinity of x_c , the coupling between the moments of the R sublattice and Co sublattice may be sensitive to the competition of the ferromagnetic Nd–Co coupling and the antiferromagnetic HR–Co coupling. The magnetization curves shown in figures 2 and 5 indicate a weak ferrimagnetic coupling between the moments of the R sublattice and the Co sublattice at a low field in the vicinity of x_c . An applied field would give rise to a complex magnetic behaviour (see figure 5) and a MMT from a weak ferrimagnetism to a strong ferrimagnetism (see figures 2 and 5). The proposed picture is consistent with the observations.

5. Conclusions

In this paper, we investigated in detail the mixing effects of light and heavy rare earth in cubic Laves phase compounds $\text{Nd}_{1-x}\text{HR}_x\text{Co}_2$ (HR = Gd, Tb) and observed some differences in magnetic properties between $\text{Nd}_{1-x}\text{Tb}_x\text{Co}_2$ and $\text{Nd}_{1-x}\text{Gd}_x\text{Co}_2$, as summarized as follows:

- (1) the concentration dependence of the lattice constant at room temperature of $\text{Nd}_{1-x}\text{Gd}_x\text{Co}_2$ presents anomalies at $x = 0.6$ due to the change of magnetic state, which is not observed in $\text{Nd}_{1-x}\text{Tb}_x\text{Co}_2$.
- (2) In $\text{Nd}_{1-x}\text{Tb}_x\text{Co}_2$, the saturation moment M_S exhibits an anomaly and can be ascribed to an abrupt jump of Co moment at $x_c \approx 0.33$. The magnetization near x_c shows complex behaviour with the variation of the applied field. Whereas in $\text{Nd}_{1-x}\text{Gd}_x\text{Co}_2$, M_S exhibits no anomaly and a relatively simple magnetic behaviour is observed near $x_c \approx 0.43$. These salient differences between these two systems can be understood by considering the structural distortion of a cubic cell at low temperature.
- (3) A field-induced MMT from a weak ferrimagnetism to a strong ferrimagnetism is observed in both compounds. This can be understood by the evolution of magnetization with the help of percolation theory.
- (4) The compensation points are observed in both systems, which are well explained within the two-sublattice model.
- (5) The AC susceptibility exhibits a double peak in the vicinity of $x_0 \approx 0.19$ for $\text{Nd}_{1-x}\text{Tb}_x\text{Co}_2$, which is not observed near $x_0 \approx 0.23$ in $\text{Nd}_{1-x}\text{Gd}_x\text{Co}_2$. Both compounds show a second-order phase transition near x_0 . The second-order phase transition could be well described by the theory of Landau phase transition. The observation of a double peak in AC susceptibility does not necessarily mean the occurrence of a first-order phase transition.

Acknowledgments

The work is supported by National Nature Science Foundation of China and by the State Key Project of Fundamental Research.

References

- [1] Goto T, Fukamichi K, Sakakibara T and Komatsu H 1989 *Solid State Commun.* **72** 945
- [2] Goto T, Sakakibara T, Murata K, Komatsu H and Fukamichi K 1990 *J. Magn. Magn. Mater.* **90/91** 700
- [3] Aleksandryan V V, Lagvtin A S, Levitin R Z, Markosyan A S and Snegirev V V 1985 *Zh. Eksp. Teor. Fiz.* **89** 271 (Engl. transl. 1985 *Sov. Phys.-JETP* **62** 153)
- [4] Saito H, Yokoyama T and Fukamichi K 1997 *J. Phys.: Condens. Matter* **9** 9333
- [5] Bartashevich M I, Aruga Katori H, Goto T, Wada H, Maeda T, Mori T and Shiga M 1997 *Physica B* **229** 315
- [6] Wada H, Mori T, Shiga M, Aruga Katori H, Bartashevich M I and Goto T 1994 *Physica B* **201** 139
- [7] Bloch D, Edwards D M, Shimizu M and Voiron J 1975 *J. Phys. F: Met. Phys.* **5** 1217
- [8] Inoue J and Shimizu M 1982 *J. Phys. F: Met. Phys.* **12** 1811
- [9] Khmelevskiy S and Mohn P 2000 *J. Phys.: Condens. Matter* **12** 9453
- [10] Adachi H and Ino H 1999 *Nature* **401** 148
- [11] Taylor J W, Duffy J A, Bebb A M, Lees M R, Bouchenoire L, Brown S D and Cooper M J 2002 *Phys. Rev. B* **66** 161319
- [12] Duc N H, Hien T D, Brommer P E and Franse J J M 1992 *J. Magn. Magn. Mater.* **104–107** 1252
- [13] Duc N H, Brommer P E and Franse J J M 1993 *Physica B* **191** 239
- [14] Gratz E, Lindbaum A, Markosyan A S, Mueller H and Sokolou A Y 1994 *J. Phys.: Condens. Matter* **6** 6699
- [15] Andreev A V 1995 *Handbook of Magnetic Materials* vol 8, ed K H J Buschow (Amsterdam: North-Holland) p 68
- [16] Swift W M and Wallace W E 1968 *J. Phys. Chem. Solids* **29** 2053
- [17] Wohlfarth E P 1968 *J. Phys. C: Solid State Phys.* **21** 68
- [18] Ouyang Z W, Rao G H, Yang H F, Liu W F and Liang J K 2002 *Appl. Phys. Lett.* **81** 97
- [19] Buschow K H J and van Stapele R P 1970 *J. Appl. Phys.* **41** 4066
- [20] Primavesi G J, Taylor K N R and Harris I R 1971 *J. Physique Coll.* **32** C1 661
- [21] Hirotsawa S and Nakamura Y 1982 *J. Magn. Magn. Mater.* **25** 284
- [22] Garcia F, Soares M R, Takeuchi A Y and de Cunha S F 1998 *J. Alloys Compounds* **279** 117

-
- [23] Duc N H and Brommer P E 1999 *Handbook of Magnetic Materials* vol 12, ed K H J Buschow (Amsterdam: North-Holland) p 259
- [24] Landau L D 1937 *Phys. Z. Sow. Un.* **11** 545
- [25] Landau L D and Lifshitz E M 1980 *Statistical Physics* 3rd edn, part 1 (Oxford: Pergamon)
- [26] Duc N H 1997 *Handbook on the Physics and Chemistry of Rare Earths* vol 24, ed K A Gschneidner Jr and L Eyring (Amsterdam: North-Holland) ch 163, p 338
- [27] Levitin R Z and Markosyan A S 1990 *J. Magn. Magn. Mater.* **84** 247
- [28] Aleksandryan V V, Levitin R Z, Markosyan A S, Snegirev V V and Shchurova A D 1987 *Sov. Phys.–JETP* **65** 502
- [29] Cullen J R and Clark A E 1977 *Phys. Rev. B* **15** 4510
- [30] Clark A E, Cullen J R, McMasters O D and Callen E R 1976 *Proc. 21st Conf. on Magnetism and Magnetic Materials (AIP Conf. Proc. No 29)* (New York: American Institute of Physics) p 192
- [31] Koon N C and Rhyne J J 1981 *Phys. Rev. B* **23** 207